Journal Pre-proof

Thermal decomposition and combustion performance of high-energy ammonium perchlorate-based molecular perovskite

Peng Deng, Huixin Wang, Xinbo Yang, Hui Ren, Qingjie Jiao

PII: S0925-8388(20)30620-4

DOI: https://doi.org/10.1016/j.jallcom.2020.154257

Reference: JALCOM 154257

To appear in: *Journal of Alloys and Compounds*

Received Date: 11 December 2019

Revised Date: 4 February 2020

Accepted Date: 9 February 2020

Please cite this article as: P. Deng, H. Wang, X. Yang, H. Ren, Q. Jiao, Thermal decomposition and combustion performance of high-energy ammonium perchlorate-based molecular perovskite, *Journal of Alloys and Compounds* (2020), doi: https://doi.org/10.1016/j.jallcom.2020.154257.

Author contributions

Peng Deng: Conceptualization, Methodology, Software, Investigation, Data Curation, Writing-Original Draft.

Huixin Wang: Methodology, Writing-Review & Editing.

Xinbo Yang: Formal analysis, Software.

Hui Ren: Resources, Writing - Review & Editing, Supervision.

Qingjie Jiao: Resources, Writing - Review & Editing, Supervision.

Thermal decomposition and combustion performance of high-energy ammonium perchlorate-based molecular perovskite

Peng Deng[1,2], Huixin Wang[1], Xinbo Yang[1], Hui Ren[1]*, Qingjie Jiao[1]

1 State Key Laboratory of Explosion Science and Technology, Beijing Institute of Technology, Beijing 100081, China

2 School of Environment and Safety Engineering, North University of China, Taiyuan 030051, China

*Corresponding author.

E-mail address: renhui@bit.edu.cn (H. Ren).

Abstract: The development of high-energy ammonium perchlorate (NH_4ClO_4, AP)-based energetic materials is of great significance for promoting their potential applications. In this study, AP-based molecular perovskite energetic materials $(H_2dabco)[NH_4(ClO_4)_3]$ were prepared via molecular assembly strategy with the facile one-pot reaction of AP, $HClO_4$ and triethylenediamine (dabco). The as-obtained sample was characterized by X-ray diffraction (XRD) and Fourier transform infrared (FT-IR). The thermal decomposition and combustion performance was investigated by thermo-gravimetric/differential scanning calorimeter (TG-DSC), high speed photography and three-dimensional FT-IR. The results showed that combined with the oxidizer perchlorate and fuel dabco at the molecular level, ternary molecular perovskite $(H_2dabco)[NH_4(ClO_4)_3]$ possessed a more stable thermal decomposition

temperature (385.0 °C) than the monocomponent AP and the heat release is also as high as 3421 $J \cdot g^{-1}$. The thermal decomposition activation energy (181.070 $kJ \cdot mol^{-1}$) of thermal decomposition of $(H_2dabco)[NH_4(ClO_4)_3]$ had been expectably reduced from the activation energy (200.259 $kJ \cdot mol^{-1}$) of high-temperature decomposition stage of AP, despite of low-temperature decomposition stage. The synergistic catalysis thermal decomposition mechanism based on the molecular perovskite structures was proposed. And the combustion performance demonstrated molecular perovskite $(H_2dabco)[NH_4(ClO_4)_3]$ had a high energy-releasing efficiency. This work provides a proof-of-principle concept for the design and fabrication of high-performance solid propellants based on molecular perovskite $(H_2dabco)[NH_4(ClO_4)_3]$.

Keywords: Molecular perovskite; $(H_2dabco)[NH_4(ClO_4)_3]$; Thermal decomposition performance; Combustion; Synergistic catalysis reaction

1 Introduction

AP, as one of the most important solid oxidizers which accounts for over 70% of the total mass of the composite propellants, plays a valuable role in the solid rocket propellant systems [1-4]. The study of thermal decomposition and combustion process of AP has attracted much attention as a hot topic of scientific researches [5,6]. Conventionally, reducing high-temperature decomposition (HTD) temperature and reaction activation energy, as well as improving apparent heat release of AP thermal decomposition could lead to a shorter ignition delay time and higher burning rate of their composite. They had a significant influence on the energy-releasing efficiency and combustion performance of these propellants ultimately [7,8]. The current researches mainly focused on the catalysts for the thermal decomposition of AP,

including metal oxide [9-11], composite catalysts [12] and so on [13-16], aiming at reducing thermal decomposition temperatures and reaction activation energy of AP. However, these non-energetic components, which were added into the propellant systems, will affect the comprehensive energy output to a certain extent [17,18]. Therefore, it is essential and desirable to introduce a new idea to design and prepare high-energy AP-based energetic materials but not additional non-energetic catalysts.

Molecular assembly strategy is a method that molecules and molecules spontaneously connect to form stable molecular aggregates by non-covalent interactions under certain conditions [19-26]. Combined with the inorganic oxidizer perchlorate and organic fuel at the molecular level, molecular assembly strategy was introduced to design and pioneer organic-inorganic hybrid molecular perovskite energetic materials with high-symmetry ternary perovskite type ABX_3 [27-30]. AP-based molecular perovskite showed the excellent detonation performances and high thermal stability due to its unique organic-inorganic oxidizer-fuel perovskite structure [31]. AP-based molecular perovskite energetic materials have attracted more and more attention, because they possessed stronger advantages and have greater potential as major components of next generation propellants than the monocomponent AP [32].

In our previous work [33,34], AP-based molecular perovskite energetic materials with unique perovskite structures have a combustible property, which is different from the general solid oxidizer AP. And they show excellent thermal decomposition abilities. Unfortunately, their thermal decomposition behavior and mechanism can't be deeply investigated. But, studying the thermal decomposition behavior and dynamics of thermal decomposition of AP-based organic-inorganic hybrid molecular perovskite is also of great significance to understand the thermal decomposition properties towards their further applications. In this paper, AP-based molecular

perovskite ($(H_2dabco)[NH_4(ClO_4)_3]$, DAP) was prepared via molecular assembly strategy with the simple one-pot reaction of AP, $HClO_4$, and dabco. The thermal decomposition behavior and dynamics of DAP were investigated and the decomposition mechanism was proposed. The ignition and combustion properties of as-obtained samples were studied. Based on the unique organic-inorganic hybrid molecular perovskite structure, DAP energetic materials showed the lower decomposition temperature 385.0 °C and higher heat release 3421 $J \cdot g^{-1}$. And the activation energy of the DAP thermal decomposition had also reduced, compared from the high-temperature decomposition process of AP. The combustion results showed DAP possessed a high energy-releasing efficiency. This work maybe offer a new understanding for AP-based molecular perovskite DAP materials towards advanced propellants in further applications.

2 Experimental

The raw material AP and $HClO_4$ solution (concentration, 70%) were obtained from Shanxi Jiangyang Chem. Eng. Co., Ltd. Commercial triethylenediamine (1,4-diazabicyclo[2.2.2]octane, $C_6H_{12}N_2$) was provided by Shanghai Aladdin Bio-Chem Technology Co., Ltd.

In a typical experimental, 0.1 mmol AP, 0.1mmol dabco, and 0.163 ml $HClO_4$ solution (0.2 mmol) were added into 20 ml deionized water together and dissolved completely at room termperature for 1 h. The samples were obtained by re-crystallization from mixed solution. The mixed solution was placed indoor at the temperature of 25 °C. The recrystallization time is 7 days. The crystal particles were filtered and washed withed alcohol several time. The DAP samples were collected and sealed before characterization. And AP/dabco solid mixture was fabricated by physical mechanical mixed with the mass ratio of 1:1 for 30 min.

A Philips X'Pert Pro X-ray diffractometer (PANalytical, Holland) was used to collect the Powder X-ray diffraction (XRD) patterns of the samples. Fourier transform infrared (FT-IR) spectra were recorded on a Thermo Scientific Nicolet iS 50 spectrophotometer (Thermo Scientific, USA). The thermal decomposition processes were carried out by a STA449F3 thermo-gravimetric/differential scanning calorimeter (Netzsch, Germany) with the different heating rates. Three-dimensional FT-IR spectra of the decomposition gaseous products were recorded in real time using a Thermo Scientific Nicolet iS 50 spectrophotometer (Thermo Scientific, USA). The ignition and combustion processes of samples were recorded by a 11 high-speed video camera (FASTCAM-APX RS, Photron, Japan), which was used to capture the combustion images of flame propagation at 1000 frames·s^{-1}. For a typical experiment, 40 ±0.5 mg of sample was pressed into a cylindrical tablet. Nitrocellulose (~2 mg) on the bottom of the sample was first ignited by external fire source and then ignited the tested samples. Once ignited, the combustion processes of the tested samples were recorded by high-speed photography devices.

3 Results and Discussion

Powder XRD was utilized firstly to analyze the crystal structures of AP and as-obtained molecular perovskite DAP, as shown in **Fig. 1**a. For component AP, the main diffraction peaks, which are located at 15.4°, 19.4°, 22.7°, 23.9°, 24.7°, 27.4°, 30.0°, and 34.6°, reflected from the planes of (101), (011), (201), (002), (210), (211), (112), and (401) for orthorhombic AP crystal [5,35], respectively. But, the XRD pattern of DAP samples obtained by molecular assembly strategy showed a clear difference from AP. Compared with the simulated XRD (CCDC:1528106), the peaks at 12.11°, 21.1°, 24.4°, 27.4°, 36.6° and 38.2° corresponded to the crystal planes (200),

(222), (400), (420), (531), and (600) of DAP. This suggested that the molecular perovskite DAP had been synthesized successfully by molecular assembly strategy.

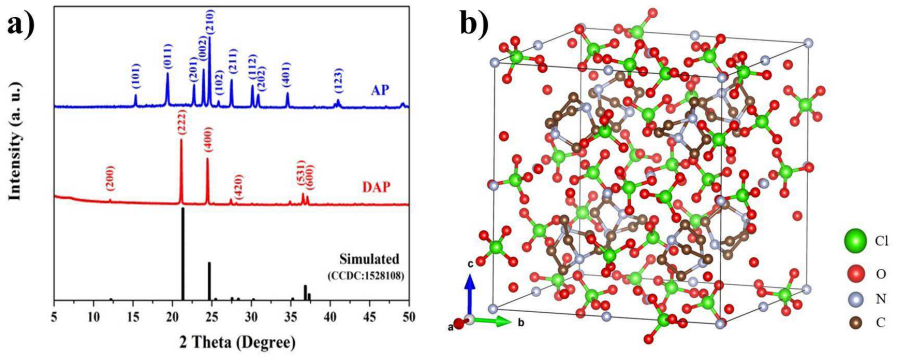

Fig. 1 (a) XRD patterns of the samples, and (b) crystal structure of DAP.

The crystal structure of molecular perovskite DAP was shown in **Fig. 1**b. In the ABX_3-type ternary molecular perovskite cell [31], protonated H_2dabco^{2+} was regarded as the A-site cation, NH_4^+ as the B-site cation, and ClO_4^- as the X-bridges. Depended on hydrogen bond and Coulomb force interactions, NH_4^+ cation, which is located on the corners, face and body centers of the cubic cell, is interacted by twelve O atoms from surrounding six ClO_4^-. And the ClO_4^- anion can be regarded as important bridge between two NH_4^+ cations here. Many strong inter-ionic hydrogen bonds are formed from O atom of ClO_4^- to H of NH_4^+, leading to forming a three-dimensional anionic cubic cage-like framework. Protonated H_2dabco^{2+} is embedded in anionic cage-like skeleton and locked by hydrogen bonds formed between H_2dabco^{2+} and ClO_4^- to promote the charge balance to zero, enhancing the stability of perovskite structure.

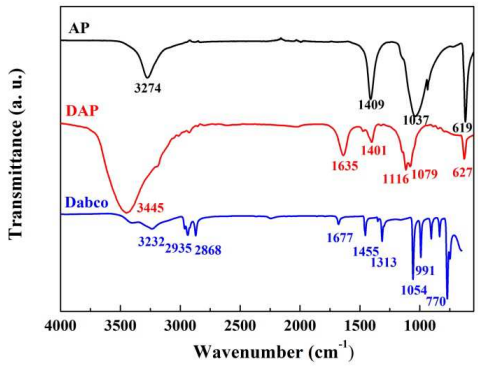

Fig. 2 FT-IR spectra of the samples

Fig. 2 shows the FT-IR spectra of the samples. The spectrum peaks located at 619 and 1037 cm^{-1} corresponded to ClO_4^-, and the peaks at 1409 and 3274 cm^{-1} to NH_4^+ from component AP. For another component dabco, the main peaks of dabco skeletal motion are located at 1054, 908, and 835 cm^{-1}. The peaks at 3235, 2937, 2870, 1678, 1455 and 991 cm^{-1} belonged to CH_2, and the peak at 1314 cm^{-1} to C-N. For DAP, the vibration peaks at 1079 and 627 cm^{-1} originated from main oxidant group ClO_4^-. The peaks of the protonated H_2dabco^{2+} skeleton at 1116, 890, and 850 cm^{-1} have a clear shifting because of hydrogen bond interactions between protonated H_2dabco^{2+} and cage-like skeleton. The above results also indicated that ternary molecule perovskite DAP have a stable chemical structure.

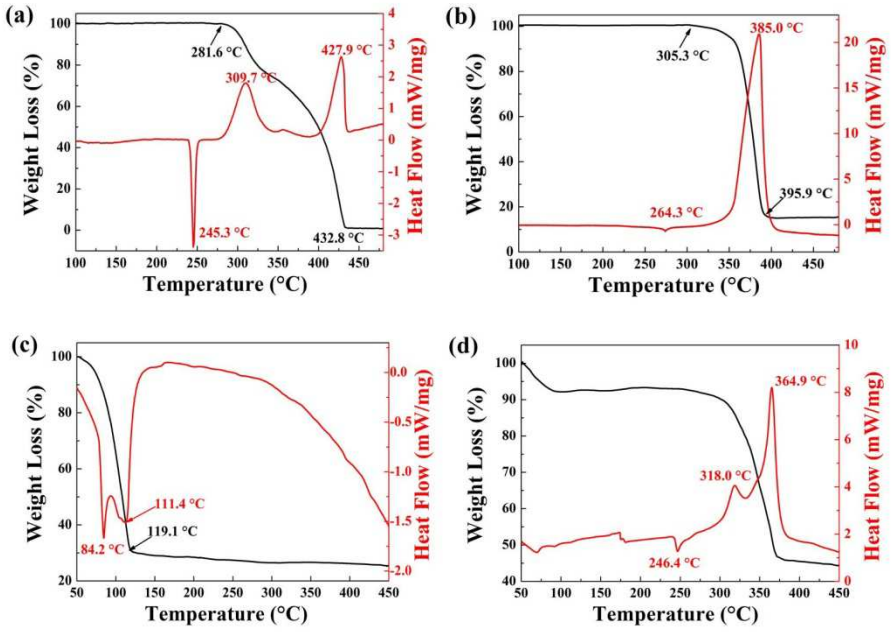

Fig.3. TG -DSC curves of (a) AP, (b) DAP, (c) dabco and (d) AP/dabco solid mixture

The thermal decomposition characteristics of the samples were investigated further. **Fig. 3**a showed the TG-DSC curve of the thermal decomposition of the monocomponent AP. The three main peaks appeared at 245.3, 309.7, and 427.9 °C can be observed. The endothermic peak at 245.3 °C corresponded to the thermotropic

phase transition of AP from orthorhombic to cubic [36]. But, the exothermic peaks at 309.7 and 427.9 °C were ascribed to the low-temperature decomposition (LTD) and HTD stages, respectively. The apparent heat release of AP during the whole decomposition process can be up to 578 $J \cdot g^{-1}$ totally, which is a good agreement with reported literatures [4,5]. During the first thermal decomposition stage, a heterogeneous process occurred with the proton transfer from NH_4^+ to ClO_4^- to form NH_3 and $HClO_4$. And then, the decomposition of $HClO_4$ would continue and produce the superoxide radical anions with the temperature raised. The NH_3 were oxidized ultimately in the second stage (high-temperature thermal decomposition), which is regarded as the key index of AP thermal decomposition.

As shown in **Fig. 3**b, DAP, integrated with inorganic oxidizer AP and organic fuel dabco in a molecular perovskite cell, have a higher onset decomposition temperature than the monocomponent AP, which is different from the decomposition processes of the monocomponent dabco and AP/dabco solid mixture in **Fig. 3** c-d. The weak endothermic peak at 264.3 °C belonged to the change of protonated H_2dabco^{2+} crystalline by thermal excitation [37]. The followed drastic decomposition process ranged from 305.3 °C to 395.9 °C in TG curve. The exothermic peak appeared at 385.0 °C. And the weight loss of the whole decomposition process is 89.6%. The value of heat release of DAP decomposition is up to 3421 $J \cdot g^{-1}$, which is higher than pure AP as well as their composite by catalyst added in **Tab. 1**. That suggested molecular perovskite DAP combined with oxidizer and fuel can release enormous heat energy by the oxidation reaction between components.

Tab. 1 Comparison of the decomposition properties of AP-based energetic materials

Sample	T_p (°C)	ΔH ($J \cdot g^{-1}$)	Ref.

AP/Graphene	322.5	2110	[38]
AP/nano-Co_3O_4	292.1	1182	[39]
AP/Fe_2O_3/graphene aergel	312.0	2383	[40]
AP/nitrated graphene oxide	350.0	3236	[41]
AP/dibenzo-18-crown-6 co-crystal	314.8	1488.4	[42]
AP/benzo-18-crown-6 co-crystal	304.2	1304.2	
AP/g-C_3N_4	384.4	1362.6	[36]
Raw AP	427.9	578	This work
DAP	385.0	3421	

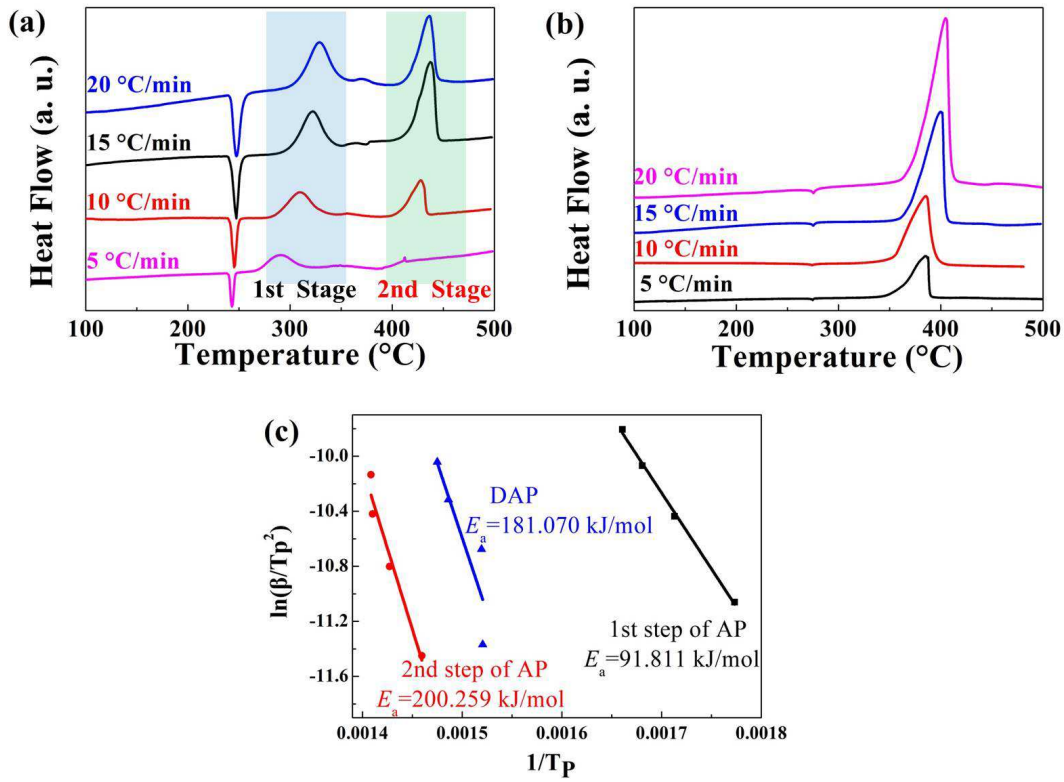

Fig.4. DSC curves of (a) AP and (b) DAP at different heating rate, (c) Dependence of $\ln(\beta/T_p^2)$ on $1/T_p$ for samples. Scatter points are experimental data and lines denotes the linear fitting results

In **Fig. 4**, the thermal decomposition dynamics of the samples were studied by DSC with different heating rates. The kinetic parameters for thermal decomposition of AP which involves the first and last decomposition stages, and DAP can be calculated by Kissinger Equation [43]:

$$\ln\frac{\beta}{T_p^{\,2}} = \ln\frac{AR}{Ea} - \frac{Ea}{RT_p} \tag{1}$$

Where β is the heating rate in degrees Celsius per minute, T_p is the peak temperature in the DSC curve at that rate. R is the gas constant, E_a is the apparent activation energy and A is the pre-exponential factor.

To the best of our knowledge, as the key index of AP thermal decomposition, the reaction activation energy (E_a) of the 2nd stage (high-temperature decomposition) was calculated to be as high as 200.259 kJ·mol^{-1}, But the lower E_a (91.811 kJ·mol^{-1}) in the 1st stage revealed that AP initiated the decomposition reaction under a lower-temperature stimuli, resulted from the intrinsic crystal structure. With a closely packed, high-symmetry ternary perovskite structure, DAP have a moderate E_a (181.070 kJ·mol^{-1}) of the decomposition stage, which decreased by 19.189 kJ·mol^{-1} from the E_a in the 2nd stage but was still higher than that of the 1st stage of AP. That demonstrated the molecular perovskite structure can enhance the thermostability of DAP energetic materials.

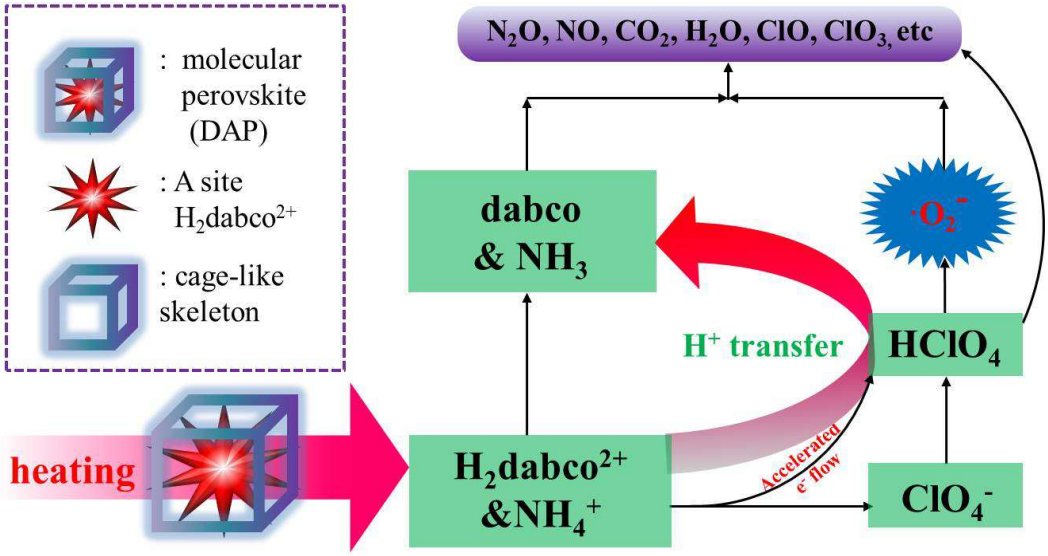

Fig. 5 Schematic of the thermal decomposition process of DAP

Based on characterization and thermal analysis results, the synergistic catalysis thermal decomposition mechanism of molecular perovskite DAP materials was provided, as shown in **Fig. 5**. Protonated H_2dabco^{2+} in the ternary system can be activated under the heating environment but can't run away from the highly heat-resistant anionic cage-like skeleton. The TG curve (**Fig. 3**b), three-dimensional FT-IR and corresponding FTIR spectra at different temperatures of DAP during the thermal decomposition process (**Fig. 6** c-d) also suggested that it was locked in the confined space originated from the stable framework structures.

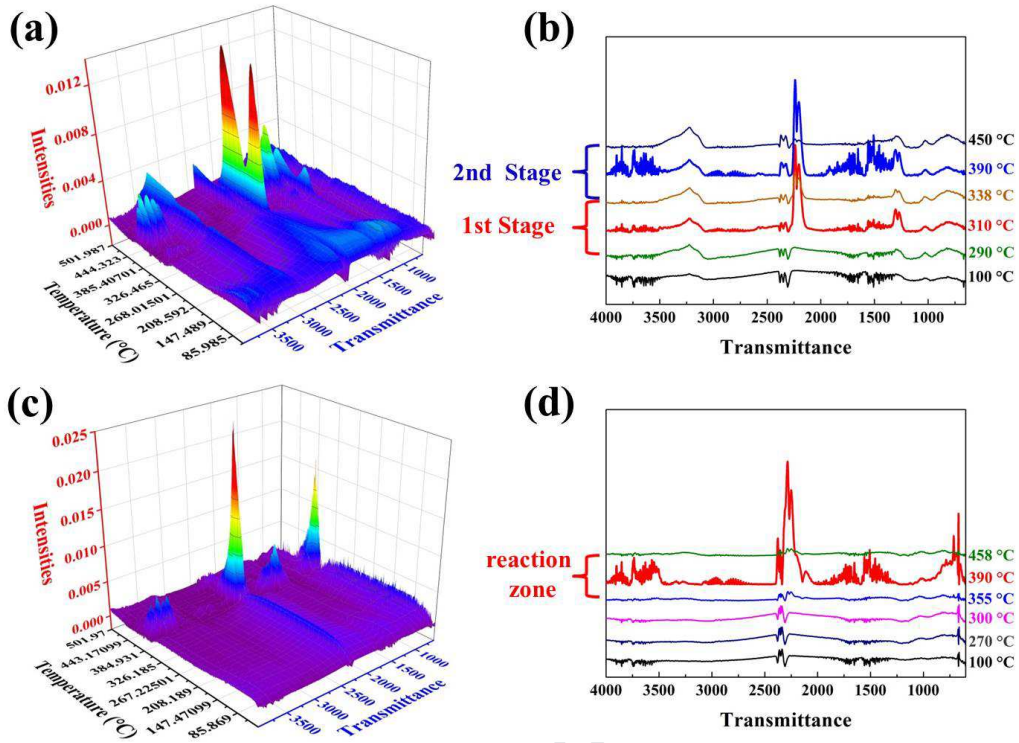

Fig. 6 Three-dimensional FT-IR spectra and corresponding FTIR spectra at different temperatures of the gaseous products of (a, c) AP and (b, d) DAP during thermal decomposition

In comparison to decomposition outgassing processes of the AP and DAP samples in **Fig. 6**, the main strongest peak positions of DAP ranged from 355 to 458 °C (**Fig. 6**d) revealed a rapid decomposition reaction process. But the triggered temperature of DAP decomposition lagged behind, compared with AP in **Fig. 6**b. It can be inferred that with the temperature raised, the anionic cage-like skeleton collapsed once a heating energy is greater than the Coulombic force between ClO_4^- and NH_4^+ of the anionic skeleton. Delayed proton transfer will occur rapidly and easily from protonated H_2dabco^{2+} and NH_4^+ to ClO_4^-, leading to the formation of $HClO_4$. Lower reaction activation energy and accelerated e^- flow from activated H_2dabco^{2+} will facilitate $HClO_4$ molecular reductive decomposition together to produce superoxide radical anion $\cdot O_2^-$. The thermogenerated $\cdot O_2^-$ can react with dabco

and NH_3 more completely to form H_2O, NO_2, N_2O, and so on. Compared from the monocomponent AP, more organic fuel (dabco) from A-sites in molecular perovskite units participated in thermal decomposition reaction, so that the more heat release energy was obtained. Namely, The unique molecular perovskite DAP combined the oxidizer and fuel can provide lower thermal decomposition activated energy and more heat release, which have more potential for the future applications.

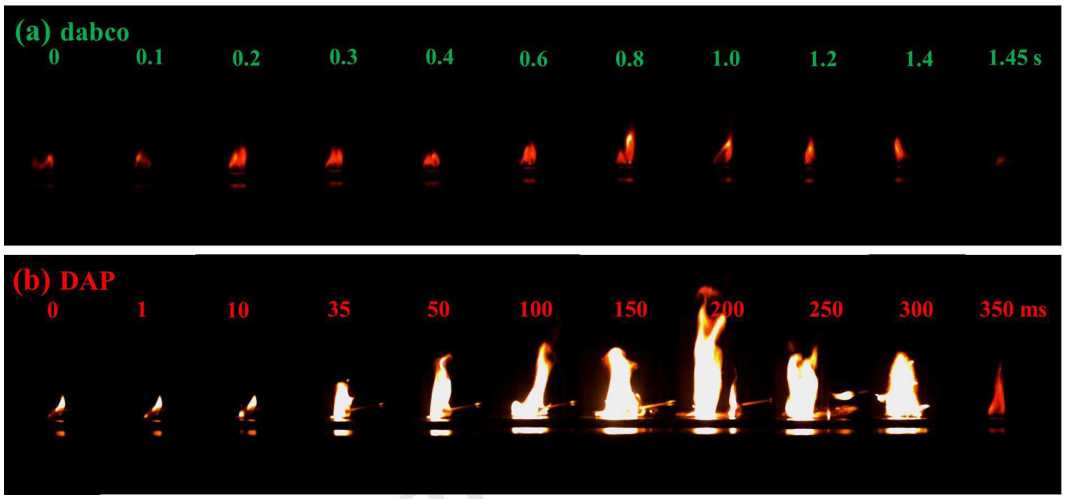

Fig. 7 The ignition and combustion process of (a) organic fuel dabco and (b) DAP

The ignition and combustion performance of DAP as well as organic fuel dabco were further investigated in **Fig 7** and **Fig. S1**. As shown in **Fig. 7a**, the combustion process of the monocomponent dabco suggested small molecules dabco can be regarded as organic fuel to join in the combustion reaction with Ignited nitrocellulose (nitrocellulose is a combustible substance as described in **Fig. S1**a) in the air. But the majority of dabco samples still remained as residual. And **Fig. S1**b showed that AP can't be directly ignited, but assist in nitrocellulose combustion where AP should be considered as a solid oxidizer. But a small amount of nitrocellulose is not enough to consume excessive AP, resulting in residue AP without reaction. The combustion process of DAP was shown in **Fig. 7**b. A sustained combustion process with violent flames can be observed from 10 to 350 ms. The short-time and fast reaction process

indicated that molecular perovskite DAP combined with organic fuel dabco and inorganic oxidizer AP can be ignited and have a fast combustion reaction rate in despite the fact that the external ignition source is not removed in time. That is because the organic fuel dabco and the inorganic oxidizer AP spontaneously assembled at a ternary cubic molecular perovskite cell to from the periodic stacking and regular crystal structures. When the trigger energy of external ignition is higher than ignition threshold of DAP, DAP was activated and ignited. As a result of close stacking of fuel and oxidizer at the molecular scale, DAP have a fierce energy-releasing effect. That demonstrated molecular perovskite DAP materials have a significant potential for in the future propellant and aerospace fields.

4 Conclusions

In summary, molecular perovskite DAP were prepared successfully via molecular assembly strategy by the facile one-pot reaction of AP, $HClO_4$, and dabco. DAP sample with perovskite structure have a more stable decomposition temperature (385 °C) than AP. The high heat release (3421 $J \cdot g^{-1}$) of DAP was obtained from the unique molecular perovskite structure combined with the inorganic oxidizer AP and organic fuel dabco. What's more, the activation energy E_a (181.070 $kJ \cdot mol^{-1}$) of DAP is lower the activation energy (200.259 $kJ \cdot mol^{-1}$) of high-temperature decomposition stage of AP. The synergistic catalysis thermal decomposition mechanism of DAP towards promoting thermal decomposition and heat energy release was proposed. This work may offer new potential for further applications of molecular perovskite energetic materials.

Acknowledgment

This work was supported by Natural Science Foundation of China (21975227, 21975024). Authors thank Prof. Weixiong Zhang and Dr. Shaoli Chen (Sun Yat-Sen University, Guangzhou, China) for help.

Appendix A Electronic supplementary information

Electronic supplementary information related to this article can be found at

References

[1] V.V. Boldyrev, Thermal decomposition of ammonium perchlorate, Thermochim. Acta 443 (2006) 1–36.

[2] X. Xiao, Z. Zhang, L. Cai, Y. Li, Z. Yan, Y. Wang, et al, The excellent catalytic activity for thermal decomposition of ammonium perchlorate using porous $CuCo_2O_4$ synthesized by template-free solution combustion method, J. Alloy. Compd. 797 (2019) 548–557.

[3] S. Isert, L. Xin, J. Xie, S.F. Son, The effect of decorated graphene addition on the burning rate of ammonium perchlorate composite propellants, Combust. Flame 183 (2017) 322–329.

[4] Q. Li, Y. He, R. Peng, One-step synthesis of SnO_2 nanoparticles-loaded graphitic carbon nitride and their application in thermal decomposition of ammonium perchlorate, New J. Chem. 39 (2015) 8703–8707.

[5] J. Chen, S. He, B. Huang, L. Zhang, Z. Qiao, J. Wang, et al., Highly space-confined ammonium perchlorate in three-dimensional hierarchically ordered porous carbon with improved thermal decomposition properties, Appl. Surf. Sci. 457 (2018) 508–515.

[6] I. Kapoor, P. Srivastava, G. Singh, Nanocrystalline transition metal oxides as catalysts in the thermal decomposition of ammonium perchlorate, Propellants Explos. Pyrotech. 34 (2009) 351–356.

[7] P. Deng, H. Ren, Q. Jiao, Enhanced thermal decomposition performance of sodium perchlorate by molecular assembly strategy, IONICS 26 (2020) 1039-1044.

[8] T. Hedman, D. Reese, K. Cho, L. Groven, R. Lucht, S. Son, An experimental study of the effects of catalysts on an ammonium perchlorate based composite Propellant using 5 kHz PLIF, Combust. Flame 159 (2012) 1748–1758.

[9] Y. Zhao, X. Zhang, X. Xu, Y. Zhao, H. Zhou, J. Li, et al. Synthesis of NiO nanostructures and their catalytic activity in the thermal decomposition of ammonium perchlorate, CrystEngComm 18 (2016) 4836–4843.

[10] M. Zou, X. Wang, X. Jiang, L. Lu, In-situ and self-distributed: A new understanding on catalyzed thermal decomposition process of ammonium perchlorate over Nd_2O_3, J. Solid State Chem. 213 (2014) 235–241.

[11] Z. Zhou, S. Tian, D. Zeng, G. Tang, C. Xie, MOX (M = Zn Co, Fe)/AP shellcore nanocomposites for self-catalytical decomposition of ammonium perchlorate, J. Alloys Compd. 513 (2012) 213–219.

[12] N. Li, Z. Geng, M. Cao, L. Ren, X. Zhao, B. Liu, et al, Well-dispersed ultrafine Mn_3O_4 nanoparticles on graphene as a promising catalyst for the thermal decomposition of ammonium perchlorate, Carbon 54 (2013) 124–231.

[13] X. Wang, J. Li, Y. Luo, M. Huang, Novel ammonium perchlorate/graphene aerogel nanostructured energetic composite: preparation and thermal decomposition, Sci. Adv. Mater. 6 (2014) 530–537.

[14] M. Kohga, Burning characteristics and thermochemical behavior of AP/HTPB composite propellant using coarse and fine AP particles, Propellants Explos. Pyrotech. 36 (2011) 57–64.

[15] G. Seyed, A. Rezgar, G. Azam, K. Abolfazl, Synthesis and characterization of α-Fe_2O_3 mesoporous using SBA-15 silica as template and investigation of its catalytic activity for thermal decomposition of ammonium perchlorate particles, Powder Technol. 278 (2015) 316–322.

[16] R. Thiruvengadathan, S. Chung, S. Basuray, B. Balasubramanian, C. Staley, K. Gangopadhyay, et al. A versatile self-assembly approach toward high performance nanoenergetic composite using functionalized graphene, Langmuir 30 (2014) 6556–6564.

[17] P. Deng, Q. Jiao, H. Ren. Synthesis of nitrogen-doped porous hollow carbon nanospheres with a high nitrogen content: A sustainable synthetic strategy using energetic precursors, Sci. Total Environ. 714 (2020) 136725.

[18] P. Deng, Y. Liu, P. Luo, J. Wang, Y. Liu, D. Wang, et al. Two-steps synthesis of sandwich-like graphene oxide/LLM-105 nanoenergetic composites using functionalized graphene. Mater. Lett. 194 (2017) 156–159.

[19] S. Sun, H. Zhang, J. Xu, S. Wang, C. Zhu, H. Wang,et al. Two novel melt-cast cocrystal explosives based on 2,4-dinitroanisole with significantly decreased melting point. Cryst. Growth Des. 2019, 19, 6826–6830.

[20] Z. Mo, H. Xu, X. She, Y. Song, P. Yan, J. Yi, et al, Constructing Pd/2D-C_3N_4 composites for efficient photocatalytic H_2 evolution through nonplasmon-induced bound electrons, Appl. Surf. Sci. 467–468 (2019) 151–157.

[21] S. Sun, H. Zhang, Y. Liu, J. Xu, S. Huang, S. Wang, et al. Transitions from Separately Crystallized CL-20 and HMX to CL-20/HMX Cocrystal Based on Solvent Media. Cryst. Growth Des. 18 (2018) 77–84.

[22] J. Lei, H. Liu, D. Yin, L. Zhou, J. Liu, Q. Chen, et al, Boosting the loading of metal single atoms via a bioconcentration strategy, Small 16 (2020) 1905920.

[23] L. Wang, X. Qu, Y. Zhao, Y. Weng, G. Waterhouse, H. Yan, et al, Exploiting single atom iron centers in a porphyrin-like MOF for efficient cancer phototherapy, ACS Appl. Mater. Interfaces 11 (2019) 35228-35237.

[24] J. Lei, Q. Guo, D. Yin, X. Cui, R. He, T. Duan, et al, Bioconcentration and bioassembly of N/S co-doped carbon with excellent stability for supercapacitors. Appl. Surf. Sci. 488 (2019) 316–325.

[25] S. Wang, F, He, X. Zhao, J. Zhang, Z. Ao, H. Wu, Phosphorous doped carbon nitride nanobelts for photodegradation of emerging contaminantsand hydrogen evolution. Appl Catal B: Environ. 257 (2019) 117931.

[26] P. Deng, Q. Jiao, H. Ren, Nano dihydroxylammonium 5,5’-bistetrazole-1,1’-diolate (TKX-50) sensitized by the liquid medium evaporation-induced agglomeration self-assembly, J. Energ. Mater. 38 (2020) doi: 10.1080/07370652.2019.1695018.

[27] T. Zuo, X. He, P. Hu, H. Jiang, Organic-inorganic hybrid perovskite single crystals: crystallization, molecular structures, and bandgap engineering, ChemNanoMat. 5 (2019) 278-289.

[28] S. Ma, M. Cai, T. Cheng, X. Ding, X. Shi, A. Alsaedi, et al. Two-dimensional organic-inorganic hybrid perovskite: from material properties to device applications, Sci. China Mater. 61 (2018) 1257-1277.

[29] S. Chen, Y. Shang, C. He, L. Sun, Z. Ye, W. Zhang, et al. Optimizing the oxygen balance by changing the A-site cations in molecular perovskite high-energetic materials, CrystEngComm 20 (2018) 7458–7463.

[30] Z. Jin, Y. Pan, X. Li, M. Hu, L. Shen, Diazabicyclo[2.2.2]octane-1,4-diium occluded in cubic anionic coordinated framework: the role of trifurcated hydrogen bonds of N–H· · ·O and C–H· · ·O, J. Mol. Struct. 60 (2003) 67–72.

[31] S. Chen, Z. Yang, B. Wang, Y. Shang, L. Sun, C. He, et al. Molecular perovskite high-energetic materials, Sci. China Mater. 61 (2018) 1123–1128.

[32] Q. Yan, F. Zhao, K. Kuo, X. Zhang, S. Zeman, L. DeLuca, Catalytic effects of nano additives on decomposition and combustion of RDX-, HMX-, and AP-based energetic compositions, Prog. Energ. Combust. Sci. 57 (2016) 75–136.

[33] X. Li, S. Hu, X. Cao, S. Hu, P. Deng, Z. Xie, Ammonium perchlorate-based molecular perovskite energetic materials: preparation, characterization, and thermal catalysis performance with MoS_2, J. Energ. Mater. 2020, Accepted. doi: 10.1080/07370652.2019.1679281

[34] P. Deng, H. Ren, Q. Jiao, Enhanced the combustion performances of ammonium perchlorate-based energetic molecular perovskite using functionalized graphene, Vacuum 169 (2019) 108882.

[35] A. Vargeese, S. Joshi, V. Krishnamurthy, Role of Poly(vinyl alcohol) in the Crystal Growth of Ammonium Perchlorate, Cryst. Growth Des. 8 (2008) 1060–1066.

[36] Q. Li, Y. He, R. Peng, Graphitic carbon nitride (g-C_3N_4) as a metal-free catalyst for thermal decomposition of ammonium perchlorate, RSC Adv. 5 (2015) 24507–24512.

[37] J. Zhou, L. Ding, F. Zhao, B. Wang, J. Zhang, Thermal studies of novel molecular perovskite energetic material $(C_6H_{14}N_2)[NH_4(ClO_4)_3]$, Chinese Chem. Lett. 31 (2020) 554–558.

[38] X. Wang, J. Li, Y. Luo, Effect of drying methods on the structure and thermal decomposition behavior of ammonium perchlorate/graphene composites, Acta Phys. Chim. Sin. 29 (2013) 2079–2086.

[39] G. Seyed, J. Seyed, B. Khosro, G. Azam, The effect of average particle size of nano-Co_3O_4 on the catalytic thermal decomposition of ammonium perchlorate particles, J. Therm. Anal. Calorim. 124 (2016) 1243–1254.

[40] Y. Lan, M. Jin, Y. Luo, Preparation and characterization of graphene aerogel/Fe_2O_3/ammonium perchlorate nanostructured energetic composite, J. Sol-Gel Sci. Technol. 74 (2015) 161–167.

[41] W. Zhang, Q. Luo, X. Duan, Y. Zhou, C. Pei, Nitrated graphene oxide and its catalytic activity in thermal decomposition of ammonium perchlorate, Mater. Res. Bull. 50 (2014) 73–78.

[42] M. Cheng, X. Liu, Q. Luo, X. Duan, C. Pei, Cocrystals of ammonium perchlorate with a series of crown ethers: preparation, structures, and properties, CrystEngComm 18 (2016) 8487–8496.

[43] L. Hu, Y. Liu, S. Hu, Y. Wang, 1T/2H multi-phase MoS_2 heterostructures: synthesis, characterization and thermal catalysis decomposition of dihydroxylammonium 5,5'-bistetrazole-1,1'-diolate, New J. Chem. 43 (2019) 10434–10441.

Research highlights:

1 Ammonium perchlorate-based organic-inorganic hybrid molecular perovskite $(H_2dabco)[NH_4(ClO_4)_3]$ was prepared via molecular assembly strategy;

2 Good thermal decomposition and combustion performance can be obtained from the perovskite-type structure;

3 The synergistic catalysis thermal decomposition mechanism of organic-inorganic hybrid molecular perovskite $(H_2dabco)[NH_4(ClO_4)_3]$ was proposed.

Declaration of Interest Statement

The authors declare no conflict of interest. The founding sponsors had no role in the design of the study; in the collection, analyses, or interpretation of data; in the writing of the manuscript, and in the decision to publish the results.

No conflict of interest.